



# Influences of Viscoelasticity and Streaming Potential on Surface Reaction Kinetics in Micro reactors

M. Fattahi<sup>1</sup>, A. Sadeghi<sup>2\*</sup>

<sup>1</sup> Department of Chemical Engineering, Petroleum University of Technology, Abadan, Iran

<sup>2</sup> Mechanical Engineering Group, University of Kurdistan, Sanandaj, Iran

**ABSTRACT:** The present study deals with investigating the influences of the streaming potential and a non-linear rheology of the carrier fluid on mass transport and surface reactions in heterogeneous microreactors. To this end, the Phan-Thien and Tanner viscoelastic model is used to predict the non-linear behavior of the fluid. The governing equations are solved in a dimensionless form utilizing the finite-difference method for a non-uniform grid. The results show that the streaming potential effects are pronounced by increasing the ionic strength of the electrolyte and thickening the electric double layer. Upon magnifying these effects, the fluid velocity and, accordingly, the speed of analyte transfer to the downstream are lowered, thereby reducing the surface reaction rates. The streaming potential effects are so severe that may lead to a 100% increase in the saturation time at limiting conditions. Although the elasticity effects decrease the saturation time by increasing the fluid velocity near the wall, they are less important as compared to the streaming potential effects.

## Review History:

Received: 4 Jun. 2018

Revised: 23 Sep. 2018

Accepted: 10 Nov. 2018

Available Online: 20 Nov. 2018

## Keywords:

Viscoelasticity

Streaming potential

Microreactor

Surface reactions

## 1- Introduction

Microreactors are among the main components of the modern lab-on-a-chip (LOC) devices. As compared with their macroscale counterparts, microreactors offer many unique advantages such as higher reaction rates [1].

The mass transport process in microreactors can be considered as a branch of solute dispersion with chemical reaction. By tracking the literature, one may come across the work of Taylor [2], as one of the landmark research works on solute dispersion. The first research work extending the dispersion problem to the situations including surface reactions was conducted by Sankarasubramanian and Gill [3].

Unlike the types of reactions occurred in chemical engineering-related fields, the reactions that take place in biological applications are usually reversible. One of the first attempts in modeling the reversible surface reactions was made by Glaser [4] who numerically investigated the kinetics of association and dissociation between a soluble analyte and an immobilized ligand.

Despite the fact that the biofluids being tested in LOCs show non-linear rheological behaviors, all the available studies pertinent to pressure-driven flow microreactors deal with Newtonian fluids. Moreover, although pressure-driven flow in micro geometries is subject to streaming potential effects, there is no study considering such effects. These gaps are filled in this study by considering the surface reaction rates in a microreactor of rectangular cross-section with a viscoelastic working fluid.

## 2- Problem Formulation

As shown in Fig. 1 and Table 1,  $H_2$  and  $H_3$  are heights of the mass transport and surface reactions in a microreactor, shown schematically in Fig. 1, is numerically studied. The flow is considered to be fully developed and the rheological behavior of the fluid is assumed to be accurately represented by the Phan-Thien and Tanner (PTT) viscoelastic model. Moreover,

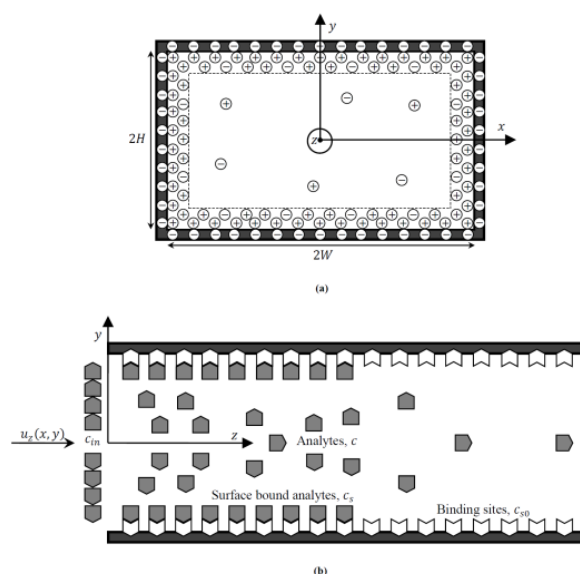


**Fig. 1. Schematic representation of the microreactor under consideration including the reactive components**

\*Corresponding author's email: a.sadeghi@eng.uok.ac.ir



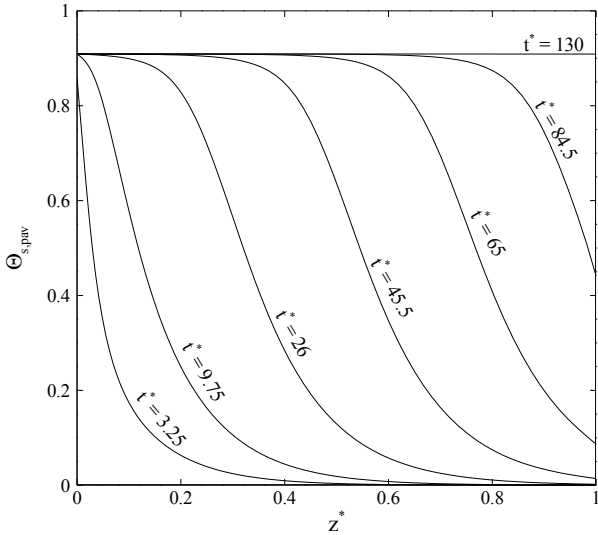


**Fig. 2. Axial variations of dimensionless perimeter-averaged concentration of surface-bound analytes at different times**

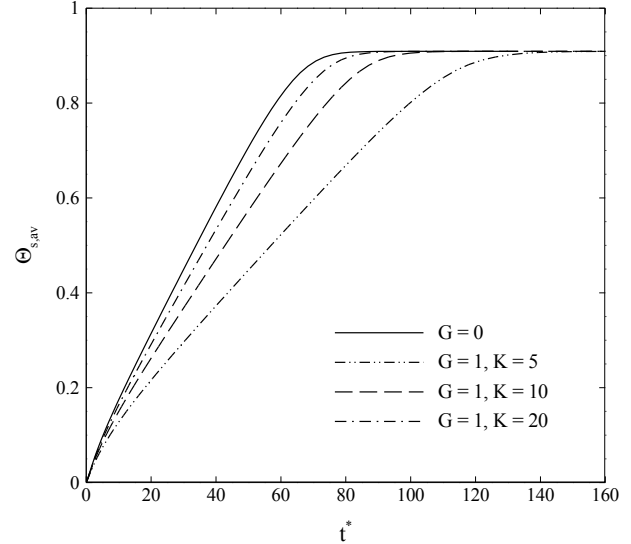


**Fig. 3. Temporal variations of the dimensionless average concentration of surface-bound analytes at different values of G and K**

it is assumed that the liquid contains a fully dissociated and symmetric salt and the wall zeta potential is uniform. It can be shown that the dimensionless governing equations under these circumstances are given as

$$\frac{\partial^2 \psi^*}{\partial x^{*2}} + \frac{\partial^2 \psi^*}{\partial y^{*2}} = K^2 \frac{\sinh \psi^*}{1 + 4\nu \sinh^2(\psi^*/2)} \quad (1)$$

$$\tau_{xz}^* = \frac{1}{\Lambda} \frac{\partial u^*}{\partial x^*}, \quad \tau_{yz}^* = \frac{1}{\Lambda} \frac{\partial u^*}{\partial y^*} \quad (2)$$

$$\Lambda = 1 + 2 \frac{\Xi We^2}{K^2} (\tau_{xz}^{*2} + \tau_{yz}^{*2}) \quad (3)$$

$$\frac{1}{\Lambda} \left( \frac{\partial^2 u^*}{\partial x^{*2}} + \frac{\partial^2 u^*}{\partial y^{*2}} \right) - \frac{1}{\Lambda^2} \left( \frac{\partial \Lambda}{\partial x^*} \frac{\partial u^*}{\partial x^*} + \frac{\partial \Lambda}{\partial y^*} \frac{\partial u^*}{\partial y^*} \right) = -2 + GE_s^* K^2 \frac{\sinh \psi^*}{1 + 4\nu \sinh^2(\psi^*/2)} \quad (4)$$

$$\frac{\partial \Theta}{\partial t^*} + u^* \frac{\partial \Theta}{\partial z^*} = \frac{\partial^2 \Theta}{\partial x^{*2}} + \frac{\partial^2 \Theta}{\partial y^{*2}} + \frac{1}{Pe^2} \frac{\partial^2 \Theta}{\partial z^{*2}} \quad (5)$$

$$\frac{\partial \Theta_s}{\partial t^*} = \Xi Da [\Theta_w (1 - \Theta_s) - K_D \Theta_s] \quad (6)$$

In these equations,  $x^* = \frac{x}{H}$ ,  $y^* = \frac{y}{H}$ ,  $z^* = \frac{z}{HPe}$ ,  $\psi^* = \frac{Ze\psi}{k_b T}$ ,  $K = H / \lambda_D$  with  $\lambda_D = (2n_0 e^2 Z^2 / \epsilon k_b T)^{-1/2}$  being the Debye length,  $\tau^* = H \tau / \mu u_{ref}$  with  $u_{ref} = -H^2 (\partial p / \partial z) / 2\mu$  denoting

the reference velocity,  $u^* = \frac{u_z}{u_{ref}}$ ,  $G = 4e^2 Z^2 n_0^2 \lambda_D^2 / \mu \lambda_m$ ,  $We = \lambda u_{ref} / \lambda_D$ ,  $\Theta = \frac{c}{c_{in}}$ ,  $\Theta_s = \frac{c_s}{c_{s0}}$ ,  $t^* = \frac{Dt_{ref}}{H^2}$ ,  $\Xi = \frac{c_m H}{c_{s0}}$ ,  $Da = \frac{k_a c_{s0} H}{D}$ ,

$K_D = \frac{k_d}{k_a c_{in}}$ , and

$$E_s^* = \frac{\int_0^1 \int_0^\alpha \frac{u^* \sinh \psi^*}{1 + 4\nu \sinh^2(\psi^*/2)} dx^* dy^*}{\alpha} \quad (7)$$

where  $\alpha = \frac{W}{H}$ . In addition, the parameter  $\nu$  is the steric factor. The set of the governing equations are solved numerically utilizing a finite-difference scheme for a non-uniform grid system subject to the pertinent boundary conditions including the prescribed zeta potential and zero velocity at the walls and the following coupling between the analyte concentration  $\Theta$  and the concentration of the surface-bound analytes  $\Theta_s$

$$\frac{\partial \Theta}{\partial x^*} \Big|_{x^*=\alpha} = -\frac{1}{\Xi} \frac{\partial \Theta_s}{\partial t^*}, \quad \frac{\partial \Theta}{\partial y^*} \Big|_{y^*=1} = -\frac{1}{\Xi} \frac{\partial \Theta_s}{\partial t^*} \quad (8)$$

Moreover, a uniform inlet concentration and a zero initial concentration are assumed.

### 3- Results and Discussion

The axial variations of dimensionless perimeter-averaged

concentration of surface-bound analytes at different times are illustrated in Fig. 2. In the beginning, the analytes only exist near the entrance; hence, the reaction only occurs in this region. Because of the high availability of the binding sites, the reaction takes place at a high rate, leading to the depletion of the solution. As time passes, the reaction rate decreases in the entrance. Furthermore, the analytes have sufficient time to reach higher axial positions. Hence, the region within which reaction occurs is extended to the downstream.

One of the main objectives of the present study is to examine the influences of the streaming potential on surface reaction rates. For a given channel, the influence of the streaming potential is dependent upon the parameters  $G$  and  $K$ . The former may be considered as the ratio of the ionic strength of the liquid to its viscosity. Hence, increasing  $G$  may be thought of as increasing the ionic strength for a given viscosity. Accordingly, it is anticipated to see lower velocities as a result of higher streaming potential effects. With increasing velocity, the analytes move slower and, hence, their presence decreases near the wall, especially at the downstream. Therefore, as observed in Fig. 3, the reaction rates decrease and more times are needed to reach the saturated state. This figure also demonstrates that a higher  $K$  is accompanied by a smaller saturation time. The reason is that the Electrical Double Layer (EDL) is thinner for a higher  $K$ , leading to lower streaming potential effects and, hence, higher fluid velocities.

It should be pointed out that the simulations showed that the saturation time is a decreasing function of both the fluid elasticity (only a weak dependence) and the steric factor but

the results are not presented for the sake of brevity.

#### 4- Conclusions

Mass transfer and surface reaction rates in a microreactor of rectangular cross-section were numerically studied. The main objective was to investigate the influences of the fluid elasticity and streaming potential on surface reaction rates. The set of the governing equations was solved utilizing a finite-difference scheme for a non-uniform grid. It was shown that the streaming potential effects may lead to significant reductions in the reaction rates. Moreover, although the saturation time was found to be a decreasing function of both the fluid elasticity and the steric factor, the impact of the former was found to be marginal.

#### References

- [1] W. Ehrfeld, V. Hessel, H. Löwe, *Microreactors: New Technology for Modern Chemistry*, Wiley, Weinheim, 2000.
- [2] G. Taylor, Dispersion of Soluble Matter in Solvent Flowing Slowly through a Tube, *Proc. R. Soc. London, Ser. A*, 219(1137) (1953) 186-203.
- [3] R. Sankarasubramanian, W.N. Gill, Unsteady Convective Diffusion with Interphase Mass Transfer, *Proc. R. Soc. London, Ser. A*, 333 (1973) 115-132.
- [4] R.W. Glaser, Antigen-antibody binding and mass transport by convection and diffusion to a surface: A two-dimensional computer model of binding and dissociation kinetics, *Anal. Biochem.*, 213(1) (1993) 152-161.

